



HAL
open science

The Role of Damping and Definition of the Robust Damping Factor for a Self-Exciting Mechanism With Constant Friction

Jean-Jacques Sinou, Guillaume Fritz, Louis Jezequel

► **To cite this version:**

Jean-Jacques Sinou, Guillaume Fritz, Louis Jezequel. The Role of Damping and Definition of the Robust Damping Factor for a Self-Exciting Mechanism With Constant Friction. *Journal of Vibration and Acoustics*, 2007, 129 (3), pp.297-306. 10.1115/1.2730536 . hal-00216085

HAL Id: hal-00216085

<https://hal.science/hal-00216085>

Submitted on 5 Oct 2018

HAL is a multi-disciplinary open access archive for the deposit and dissemination of scientific research documents, whether they are published or not. The documents may come from teaching and research institutions in France or abroad, or from public or private research centers.

L'archive ouverte pluridisciplinaire **HAL**, est destinée au dépôt et à la diffusion de documents scientifiques de niveau recherche, publiés ou non, émanant des établissements d'enseignement et de recherche français ou étrangers, des laboratoires publics ou privés.

The Role of Damping and Definition of the Robust Damping Factor for a Self-Exciting Mechanism With Constant Friction

J.-J. Sinou¹
e-mail: jean-jacques.sinou@ec-lyon.fr

G. Fritz

L. Jézéquel

Laboratoire de Tribologie et Dynamique des
Systèmes UMR-CNRS 5513,
Ecole Centrale de Lyon,
36 avenue Guy de Collongue,
69134 Ecully Cedex, France

This paper presents a linear two-degree-of-freedom model in order to analyze friction-induced instabilities that are governed by modal interaction. The role of structural damping on flutter instability is undertaken, and the effects of the structural damping ratio between the stable and unstable modes are investigated in order to clarify and to explain the mechanical process of flutter instability. In certain conditions, it is demonstrated that the merging scenario and the unstable mode may change due to this structural damping ratio. Discussions not only demonstrate the role of structural damping and the associated mechanical process but also define the robust damping factor in order to avoid design errors and to reduce flutter instability.

1 Introduction

Noise generated by friction is one of the first sources of discomfort in the field of friction-induced vibration and has been a major concern of the scientific community for quite a long time. Instabilities and the associated retained mechanism are generally divided into two main categories [1]: the first considers the “stick-slip” phenomena, whereas the second focuses on mode coupling. In the first case, self-excited vibrations may be due to the variation of the coefficient of friction with relative speed or higher static friction coefficient than dynamic. This stick-slip phenomenon induces adhering and sliding phases [2]. Effectively, when the friction coefficient is a decreasing function of the relative speed (i.e., negative slope in the friction-velocity curve), the mechanical system may have negative damping. Consequently, unstable vibrations may be generated [1,3]. As explained by Crolla and Lang [4] and Earles and Lee [5], this mechanism is recognized as explaining some friction-induced vibration problems in many earlier references. However, it was clearly observed that unstable oscillations may occur even with a constant friction coefficient. The first minimal model to demonstrate that mechanical models may give instabilities with a constant friction coefficient was developed by Spurr [6] and was called the “sprag-slip” model. Then, several workers increased the model of Spurr. For example, North [7] was the first researcher that considers brake squeal as a flutter instability with a constant brake friction. Actually, the mechanism of mode coupling for self-excited friction-induced oscillations is applied in a broad variety of engineering applications, such as automobile brake noise [3,8,9] or aircraft brake systems [10,11]. As explained by Chambrette and Jézéquel [12] and Hoffmann and Gaul [13], a two-degree-of-freedom model may be sufficient in order to investigate the mode-coupling instability in a mechanical system. We refer the interested reader to [1,3,14] for an extensive overview of friction-induced vibration in mechanical systems.

However, it may be observed that the last phenomenon, defined as a flutter instability where two modes are closer, is not yet fully understood. More particularly, the role of damping on the stabil-

ity of dynamical systems is not totally clarified. In 1987, Earles and Chambers [15] proposed to include disk damping for a double-pin and disk system in order to undertake the concept of the mechanism of disk brake squeal noise generation. They observed that increasing damping not only has a general tendency to decrease instability intensity, but also has the effect of increasing the size of the unstable region for certain physical parameters. They concluded that damping influences the prediction of stable-unstable motions, but that it is not possible to make predictions intuitively.

Recently, some researchers [13,16–18] demonstrated that the role of damping is very important and that the addition of damping may make the dynamical system worse: they concluded that an increase in damping in order to stabilize friction-induced vibrations may be incorrect. For example, Shin et al. [16,17] showed that adding damping to either the disk or the pad of the brake system may make the system more unstable. Moreover, Hoffmann and Gaul [13] proposed to develop a two-degree-of-freedom model and a feedback-loop formalism in order to investigate qualitative and quantitative aspects of the mode-coupling instability in the presence of structural damping and to understand the associated mechanical processes. They concluded that the effects of damping on mode-coupling instability in friction-induced vibrations is a surprising and complex phenomenon. Then, Sinou and Jézéquel [18] resumed this study and demonstrated that structural damping is essential and affects not only the stability of mechanical systems subject to friction-induced vibration but also the evolution of the limit-cycle amplitudes. These recent studies [13,18] concluded that considering the undamped associated system may be incorrect in order to undertake stability analysis of mechanical systems. Structural damping is one of the primary parameters in flutter instabilities and may not be ignored in order to design mechanical systems, such as automotive brake or train wheels, for example.

Considering all these recent developments on mode-coupling friction-induced instability and industrial demands for design, it is important at this stage to assess the sensitivity of stability to structural damping and to be able to explain the mechanical process in order to define the more adequate structural damping for mechanical systems. The objective of this present work is to investigate

¹Corresponding author.

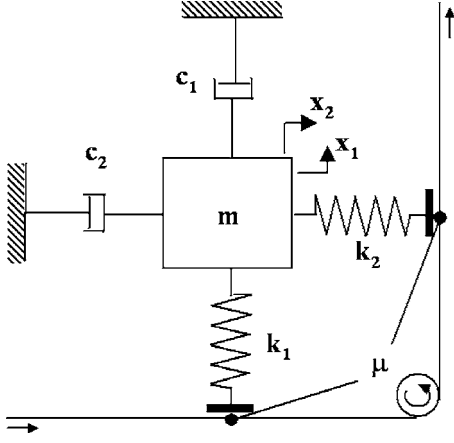


Fig. 1 Mechanical system

these last points in order to define the most efficient structural damping, called the robust damping factor (RD-factor) for flutter instability.

First of all, a simple two-degree-of-freedom system with friction will be presented in order to examine the role of damping on mode-coupling instability. Second, the effects of structural damping will be clarified and the associated mechanical process will be clearly identified: the role and evolution of the stable and unstable modes will be examined in detail.

Then, the definition of the (RD-factor) for mechanical systems subject to flutter instability will be introduced. It will be demonstrated that the structural damping ratio between the stable and unstable modes is essential and that, even if the role of damping is one of the most important physical parameters in flutter instability, its interaction and effects with the evolutions of others parameters may be taken into account to avoid design errors.

2 Mechanical System

The mechanical system under study, shown in Fig. 1 is composed of a mass held against a moving band. For the sake of simplicity, we assume that the mass and band surfaces are always in contact. Physically speaking, this assumption may be due to a preload applied to the system. The contact between the mass and the band is modeled by two plates supported by two different springs.

This model, first introduced by Hultén [19,20] and resumed by Sinou and Jézéquel [18], does not intend to capture all geometrical properties of any real system with friction interfaces, but has been chosen due to its simplicity in order to investigate friction-induced vibration and to better understand the roles and effects of various physical parameters including more specifically the damping.

Concerning the friction forces between the two plates and the band, the Coulomb's law is assumed

$$T = \mu N \quad (1)$$

where T and N define the tangential and normal forces and μ is the coefficient of friction that is assumed to be constant. Finally, it is assumed that the direction of friction force does not change due to the fact that the relative velocities between the band speed and the displacements of the mass are assumed to be positive.

The resulting equations of motion can be written in matrix form as [18]

$$\begin{bmatrix} 1 & 0 \\ 0 & 1 \end{bmatrix} \begin{pmatrix} \ddot{X}_1 \\ \ddot{X}_2 \end{pmatrix} + \begin{bmatrix} \eta_1 \omega_{0,1} & 0 \\ 0 & \eta_2 \omega_{0,2} \end{bmatrix} \begin{pmatrix} \dot{X}_1 \\ \dot{X}_2 \end{pmatrix} + \begin{bmatrix} \omega_{0,1}^2 & -\mu \omega_{0,2}^2 \\ \mu \omega_{0,1}^2 & \omega_{0,2}^2 \end{bmatrix} \begin{pmatrix} X_1 \\ X_2 \end{pmatrix} = \begin{pmatrix} 0 \\ 0 \end{pmatrix} \quad (2)$$

Table 1 Value of the physical parameters

Notation	Description	Value
$\omega_{0,1}$	first natural pulsation	$2\pi \times 100$ rad/s
$\omega_{0,2}$	second natural pulsation	$2\pi \times 75$ rad/s
m	mass	1 kg

where X_1 and X_2 are the relative displacements indicated in Fig. 1. This mechanical system may become unstable due to the stiffness matrix that is asymmetric and the associated mechanical process will be defined as a result of the friction force. $\omega_{0,i}$ defines the i th natural pulsation

$$\omega_{0,i} = \sqrt{\frac{k_i}{m}} \quad (3)$$

and η_i defines the i th relative damping coefficient

$$\eta_i = \frac{c_i}{\sqrt{k_i m}} \quad (4)$$

Stability analysis is investigated by considering eigenvalues of the characteristic equation

$$\det(\lambda^2 \mathbf{M} + \lambda \mathbf{C} + \mathbf{K}) = 0 \quad (5)$$

where \mathbf{M} , \mathbf{C} , and \mathbf{K} are the mass, damping, and stiffness matrices, respectively, of the dynamical system (2). Then, the system is stable if all the real parts of eigenvalues are inferior to zero

$$\forall \lambda \operatorname{Re}(\lambda) \leq 0 \quad (6)$$

and unstable if there exist one or more eigenvalues having a real part superior to zero

$$\exists \lambda \operatorname{Re}(\lambda) > 0 \quad (7)$$

3 Stability Analysis and Numerical Results

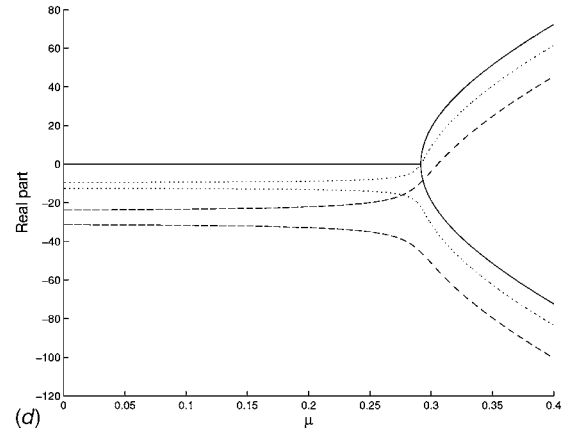
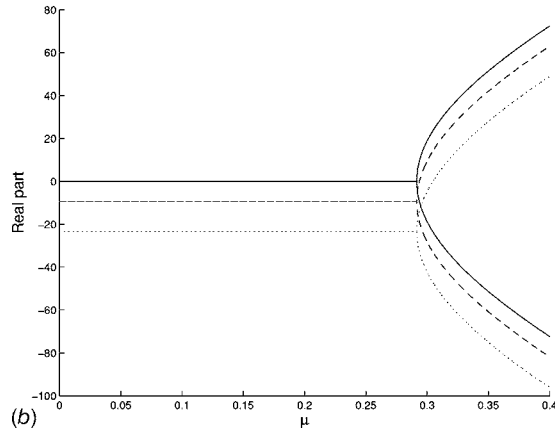
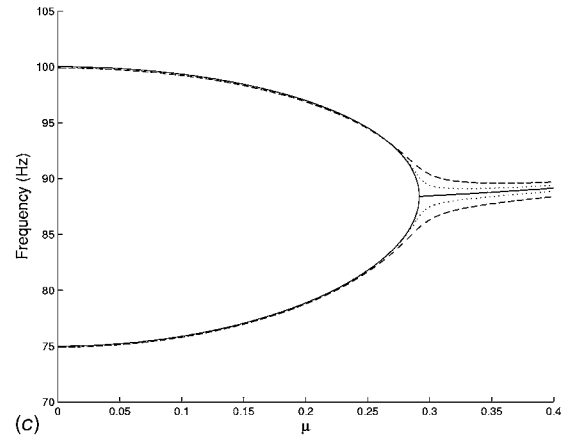
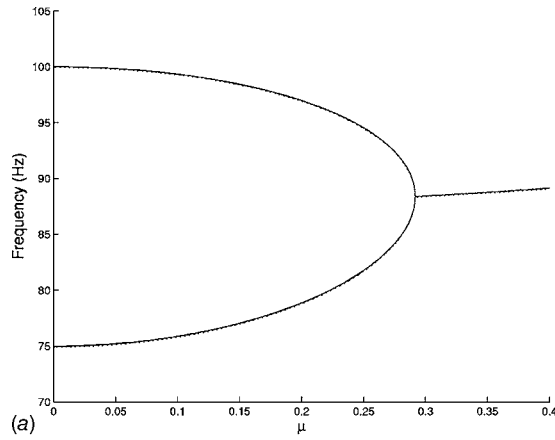
In this section, some numerical results are presented based on the previous system 1. The used physical parameters are defined in Table 1.

In order to investigate the role of structural damping, two physical cases will be studied: the first case considers proportional damping ($c_1 = c_2$, i.e., $\omega_{0,1} \eta_1 = \omega_{0,2} \eta_2$) and the second nonproportional damping ($c_1 \neq c_2$, i.e., $\omega_{0,1} \eta_1 \neq \omega_{0,2} \eta_2$) between the two modes. Then, the effects of the structural damping ratio will be undertaken.

3.1 Effects of Proportional Structural Dampings. First, the effects of structural damping are undertaken and the associated physical mechanical process will be explained. Figures 2(a) and 2(b) illustrate the effect of increasing proportional damping: the change in the real and imaginary parts of eigenvalues against the friction coefficient μ is studied for three proportional structural dampings, as indicated in Table 2.

It may be observed that the merging of the two modes appears to be perfect in the case of proportional damping: the stable and unstable modes have exactly the same frequency, as shown in Fig. 2(a). Moreover, adding proportional damping increases the value of the Hopf bifurcation control parameter μ_0 for which the instability appears (as illustrated in Fig. 2(b)). Effectively, the real parts of eigenvalues cross the zero real-part axis for higher value of the friction coefficient due to the fact that the real parts' curves run toward the negative real parts. In this case, the frequencies of the stable and unstable modes are not very little affected, as illustrated in Figure 2(a).

In conclusion, a generally condition (but not sufficient) to enhance the stability of a mechanical system is that proportional structural damping is added to both the unstable and stable modes. This is a very well-known result for friction-induced flutter instability.



$$d^4 + 2d^3 + (c_{0,1}^2 + c_{0,2}^2 + d^2)^2 + (c_{0,1}^2 + c_{0,2}^2)d + c_{0,1}^2 c_{0,2}^2 (1 + \nu^2) = 0$$

This result may be demonstrated by considering the previous analytical expressions of the system. Effectively, the stability of the system is driven by Eq. (5), in which structure depends on the presence of damping. Indeed, once expanded, Eq. (5) gives

$$d^4 + (\bar{\mathcal{E}}_1 c_{0,1} + \bar{\mathcal{E}}_2 c_{0,2})^3 + (c_{0,1}^2 + c_{0,2}^2 + \bar{\mathcal{E}}_1 c_{0,1} \bar{\mathcal{E}}_2 c_{0,2})^2 + (\bar{\mathcal{E}}_1 c_{0,1} c_{0,2} + \bar{\mathcal{E}}_2 c_{0,2} c_{0,1}) + c_{0,1}^2 c_{0,2}^2 (1 + \nu^2) = 0 \quad (8)$$

The first- and third-order terms of this polynomial exist only in case of damping. Here, we focus on two case studies corresponding to the equally damped and the undamped equations. Here, we aim at investigating the relationship between these two configurations, which are respectively defined as $\bar{\mathcal{E}}_1 c_{0,1} = \bar{\mathcal{E}}_2 c_{0,2} = d$ and $\bar{\mathcal{E}}_1 c_{0,1} = \bar{\mathcal{E}}_2 c_{0,2} = 0$. As shown in Fig. 2(a) and 2(b), this study is motivated by the fact that these two configurations seem numerically to give results that are close to each other, with a shift in real parts. Assuming \tilde{s} to be the solution of the equally damped equation,

$$d^4 + 2d^3 + (c_{0,1}^2 + c_{0,2}^2 + d^2)^2 + (c_{0,1}^2 + c_{0,2}^2)d + c_{0,1}^2 c_{0,2}^2 (1 + \nu^2) = 0 \quad (9)$$

Let \tilde{s} be solution of the undamped equation

$$d^4 + (c_{0,1}^2 + c_{0,2}^2)^2 + c_{0,1}^2 c_{0,2}^2 (1 + \nu^2) = 0 \quad (10)$$

Equation (10) features only even order terms. We aim at assessing if \tilde{s} , shifted in real part, may be solution of an equation of the kind of Eq. (10) with a modified stiffness. Therefore, we will assume: $\tilde{s} = s + R/\nu$. It leads to

$$d^4 + 4s^3 + (\tilde{c}_{0,1}^2 + \tilde{c}_{0,2}^2 + 6s^2)^2 + (2s(\tilde{c}_{0,1}^2 + \tilde{c}_{0,2}^2) + 4s^3) + \tilde{c}_{0,1}^2 \tilde{c}_{0,2}^2 (1 + \nu^2) + s^4 + s^2(\tilde{c}_{0,1}^2 + \tilde{c}_{0,2}^2) = 0 \quad (11)$$

The tilde is for the modified stiffness. Then a term-by-term identification between Eqs. (9) and (11) gives

$\bar{\mathcal{E}}_1$	$\bar{\mathcal{E}}_2$	c_1 (N s m ⁻¹)	c_2 (N s m ⁻¹)
0.0187	0.025	23.56	23.56
0.0375	0.05	47.12	47.12

$\bar{\mathcal{E}}_1$	$\bar{\mathcal{E}}_2$	c_1 (N s m ⁻¹)	c_2 (N s m ⁻¹)
0.05	0.05	62.83	47.12
0.025	0.025	31.42	23.56

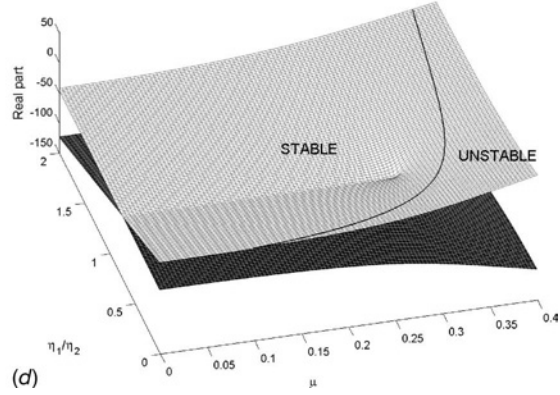
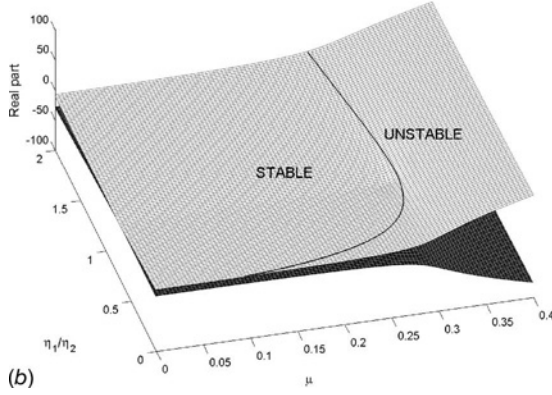
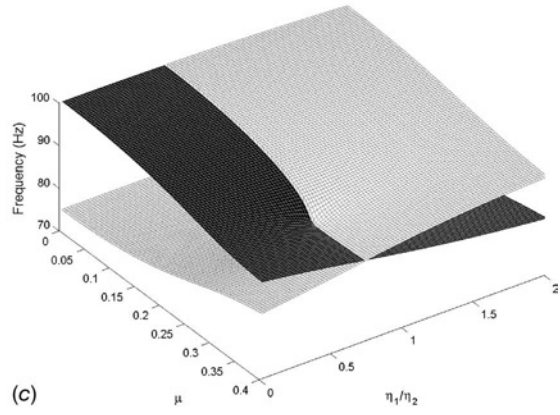
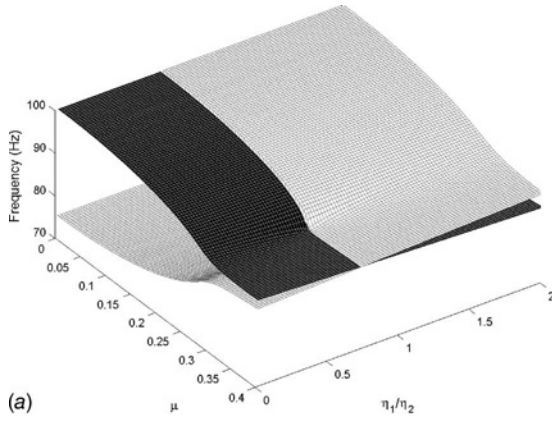


Table 3
 η_1/η_2 0.02, 0.1

1 2 0 0

$$\begin{cases} 2d = 4s \\ \tilde{c}_{0,1}^2 + \tilde{c}_{0,2}^2 + d^2 = \tilde{c}_{0,1}^2 + \tilde{c}_{0,2}^2 + 6s^2 \\ (\tilde{c}_{0,1} + \tilde{c}_{0,2})d = 2s(\tilde{c}_{0,1} + \tilde{c}_{0,2}) + 4s^3 \\ \tilde{c}_{0,1}^2 \tilde{c}_{0,2}^2 (1 + \nu^2) = \tilde{c}_{0,1}^2 \tilde{c}_{0,2}^2 (1 + \nu^2) + s^4 + s^2(\tilde{c}_{0,1}^2 + \tilde{c}_{0,2}^2) \end{cases} \quad (12)$$

We now have to check whether this system is consistent or not. First, we can note that the third equation is linked with the first and second ones. Thus, Eq. (12) may be rewritten as follows:

$$\begin{cases} s = \frac{d}{2} \\ \tilde{c}_{0,1}^2 + \tilde{c}_{0,2}^2 = \tilde{c}_{0,1}^2 + \tilde{c}_{0,2}^2 - \frac{d^2}{2} \\ \tilde{c}_{0,1}^2 \tilde{c}_{0,2}^2 = \tilde{c}_{0,1}^2 \tilde{c}_{0,2}^2 - \frac{d^2}{4(1 + \nu^2)} \left(\tilde{c}_{0,1}^2 + \tilde{c}_{0,2}^2 - \frac{d^2}{4} \right) \end{cases} \quad (13)$$

It means that if s is solution of the equally damped equation with nominal stiffness $(\tilde{c}_{0,1}, \tilde{c}_{0,2})$, then $s + d/2$ is the solution of the undamped equation with modified stiffness $(\tilde{c}_{0,1}, \tilde{c}_{0,2})$ defined in Eq. (13).

3.2 Effects of Nonproportional Structural Damping. Second, the effects of nonproportional structural damping ($c_1 \in c_2$, i.e., $\tilde{c}_{0,1} \tilde{c}_{0,2} \in \tilde{c}_{0,2} \tilde{c}_{0,1}$) between the two modes is undertaken. Figures 2(c) and 2(d) illustrate the effect of increasing nonproportional damping: the change in the real and imaginary parts of eigenvalues against the friction coefficient ν is studied for three nonproportional structural damping, as indicated in Table 3.

Figures 2(c) and 2(d) indicate that the merging is imperfect in

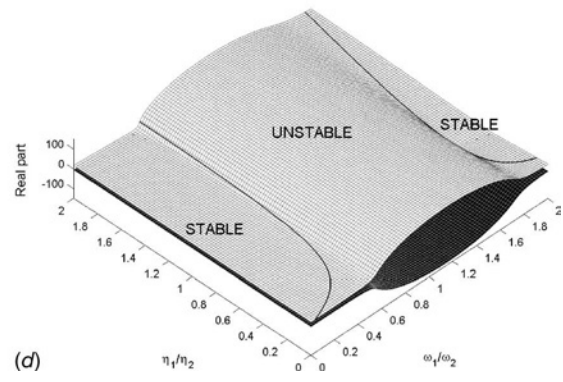
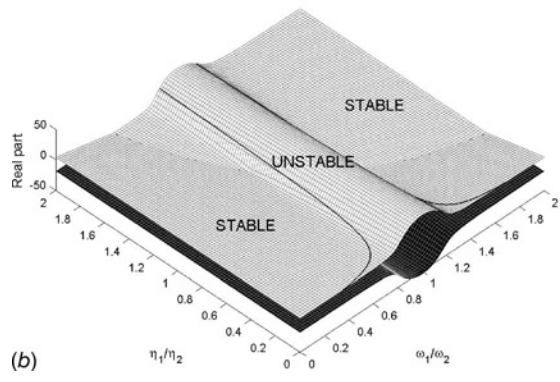
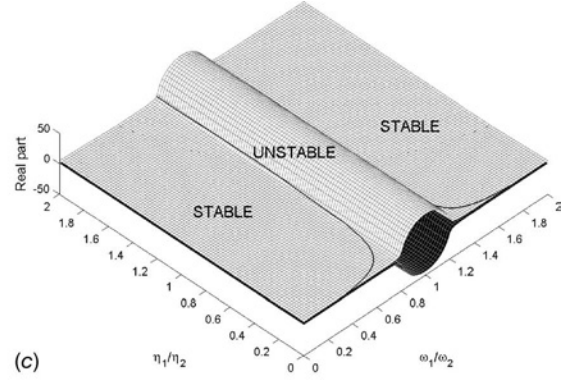
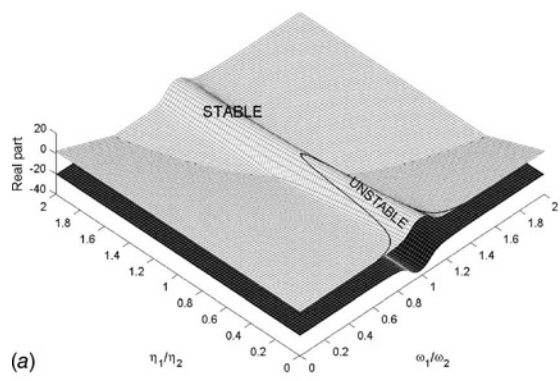
the case of nonproportional structural damping. The difference between the stable and unstable frequencies depends of the structural damping ratio between the two modes (as shown in Figure 2(c)).

It may be observed that the evolution of the real part for the proportional and nonproportional structural damping is different. In the case of proportional structural damping, the evolution of the real part (for the stable and unstable modes) only appears at the Hopf bifurcation point of the undamped system. In the case of nonproportional damping, the real parts of the stable and unstable modes increase and decrease, respectively, with the evolution of the friction coefficient.

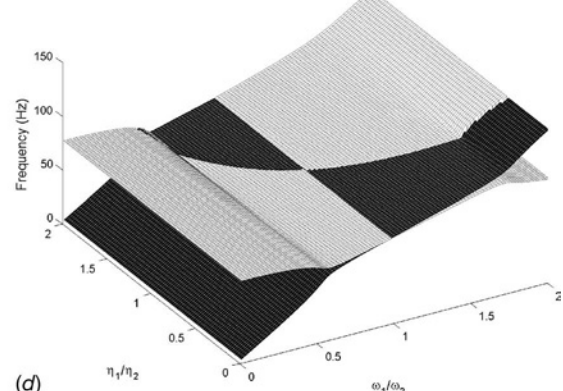
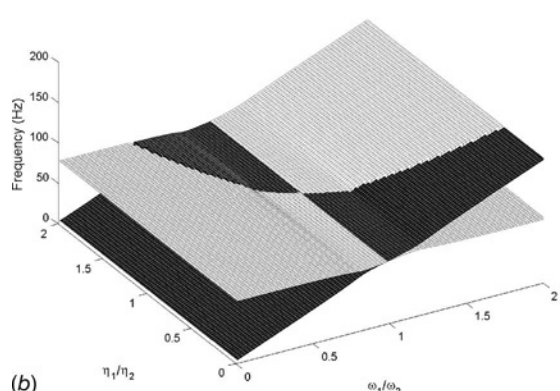
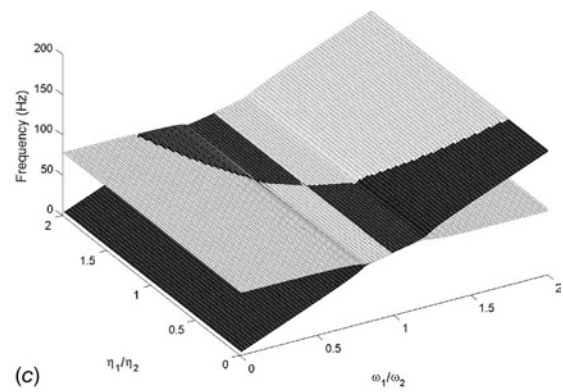
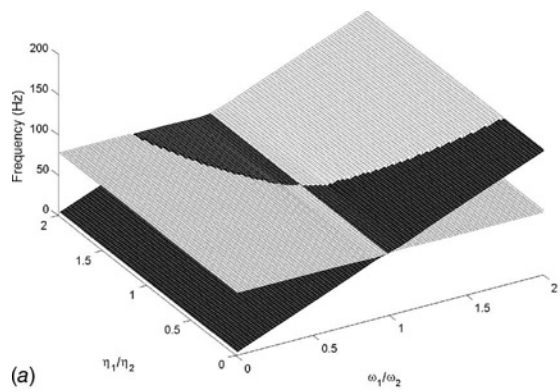
3.3 Effects of Structural Damping Ratio. Considering the previous results, it appears that the role of structural damping is essential and cannot be neglected. Moreover, the structural damping ratio between the two modes seems to be important. In this section, the role of the structural damping ratio will be undertaken.

Figures 3 illustrates the evolution of the real parts and frequencies versus the damping ratio \tilde{c}_1/\tilde{c}_2 and the friction coefficient ν for two values of the structural damping \tilde{c}_2 . Increasing the structural damping \tilde{c}_2 (for a given value of structural damping \tilde{c}_1) reduces the unstable region and has little effect on the gap between the frequencies of the stable and unstable modes. However, the classical result that increasing damping in only one part of the system may induce mode-coupling instability is always observed.

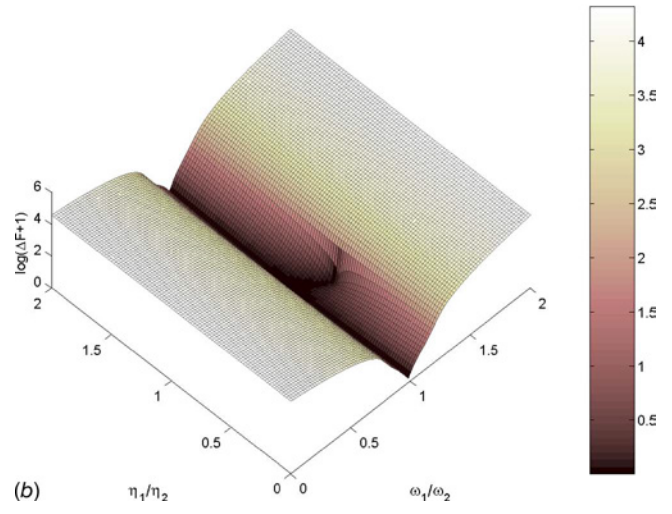
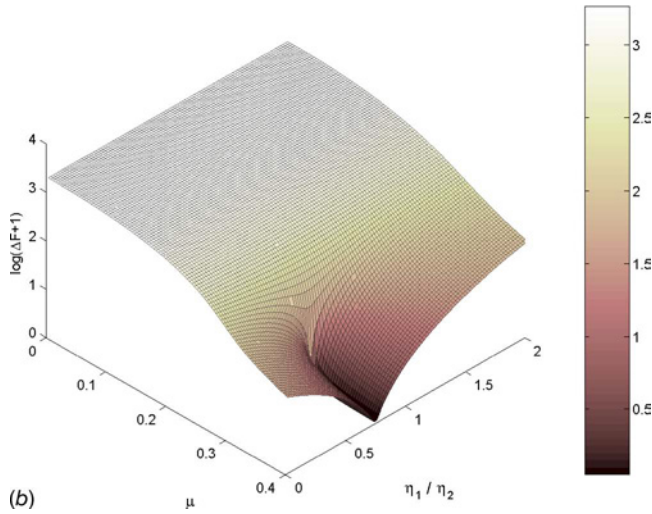
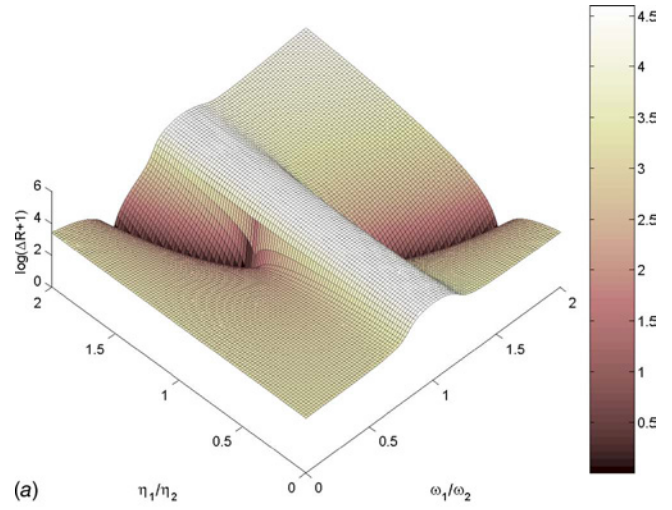
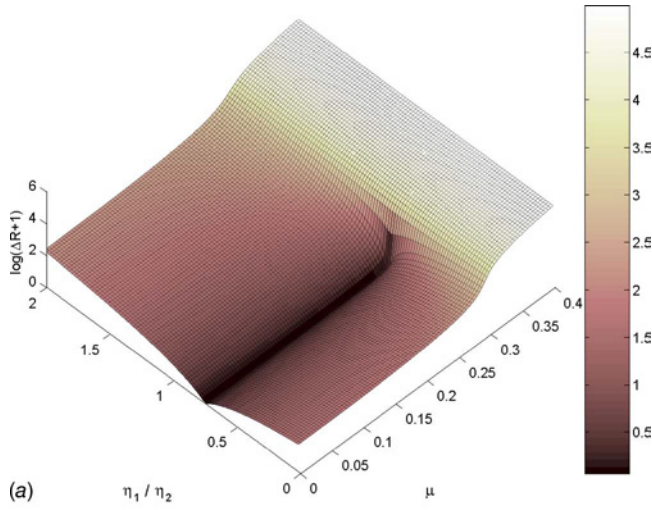
A particular observation is the evolution of the stable and unstable modes with the variation of the structural damping ratio \tilde{c}_1/\tilde{c}_2 . In order to undertake and to clarify the effects of structural damping on flutter instability, evolutions of the two modes that merge if the system is unstable are defined as follows: the black



η_1/η_2 0.1 0.2 0.1 0.2 0.1 0.2 0.02,
 ω_1/ω_2 0.1 0.2 0.1 0.2 0.1 0.2 0.02,



η_1/η_2 0.1 0.2 0.1 0.2 0.1 0.2 0.02,
 ω_1/ω_2 0.1 0.2 0.1 0.2 0.1 0.2 0.02,



0.7 0.1 0.2 1 1 0.2 0.1

0.7 0.1 0.2 1 1 0.2 0.1

surface (for both the evolution of the frequency and real part) is associated with the stable static solution of the merging scenario; the white surface corresponds to the evolution of the mode associated with the static solution that becomes unstable after the Hopf bifurcation point. Using this surface color, it is possible to follow the effect of damping on the stable and unstable modes and the associated merging scenario. Then, a fundamental understanding of the flutter instability process can be shown. Increasing or decreasing the structural damping ratio $\bar{\mathcal{E}}_1/\bar{\mathcal{E}}_2$ changes the merging scenario of flutter instability. When the damping ratio $\bar{\mathcal{E}}_1/\bar{\mathcal{E}}_2$ is such that

$$\frac{\bar{\mathcal{E}}_1}{\bar{\mathcal{E}}_2} \approx \frac{0.2}{0.1} \text{ (i.e. } c_1 = c_2) \quad (14)$$

the stable mode becomes unstable and the unstable mode becomes stable.

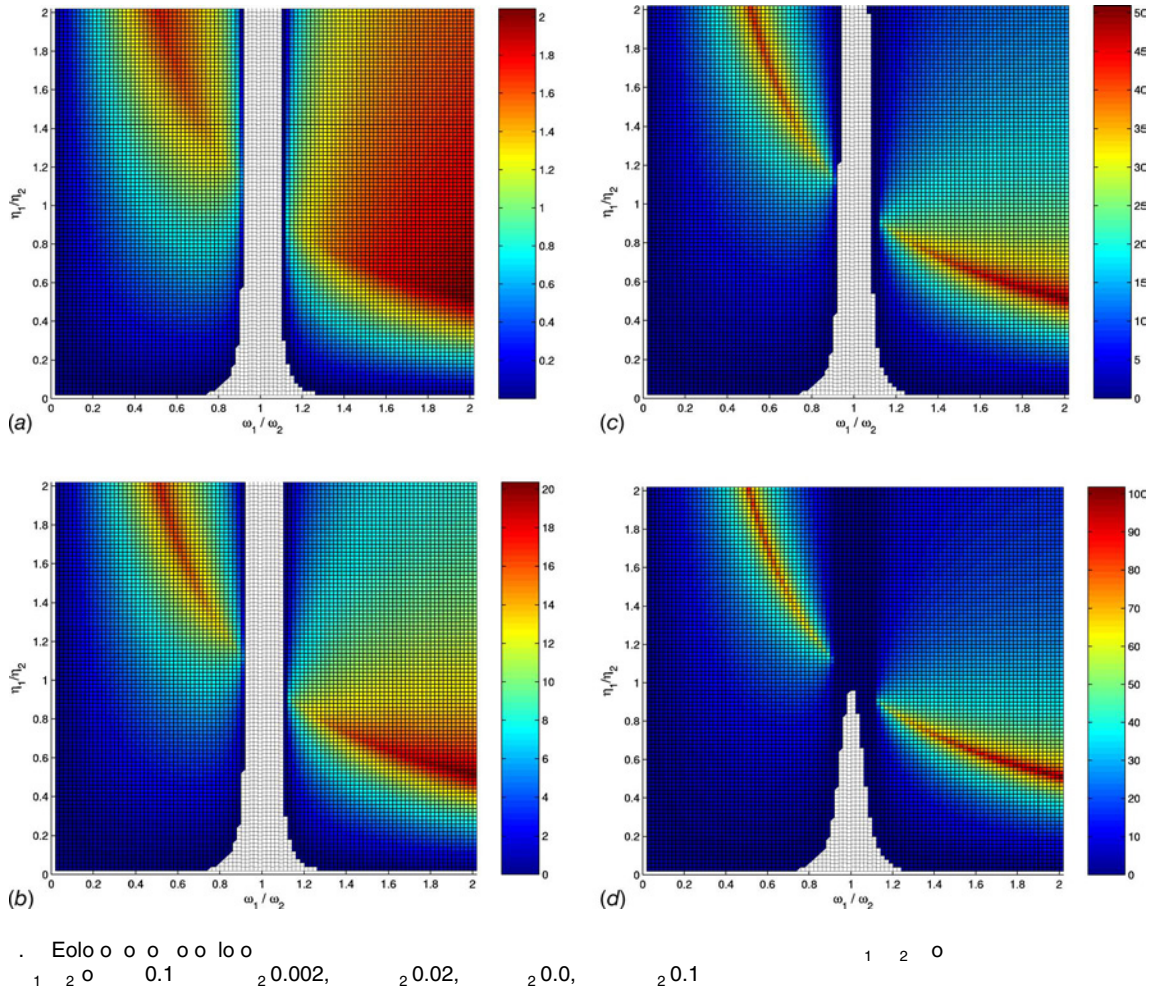
In Figs. 3(a) and 3(b) (corresponding to $\bar{\mathcal{E}}_2=0.02$), it may be observed that the optimal value of the damping ratio $\bar{\mathcal{E}}_1/\bar{\mathcal{E}}_2$ (which defines the more stable system in relation to this damping ratio) corresponds to the change in the unstable and stable behavior for the two coupling modes. In this case, the value of this optimal damping ratio corresponds to Eq. (14).

However, this last phenomenon is not observed in the case of higher damping (see Figs. 3(c) and 3(d), corresponding to $\bar{\mathcal{E}}_2=0.1$). Here, the stable area increase when the damping ratio

$\bar{\mathcal{E}}_1/\bar{\mathcal{E}}_2$ increases even if the merging scenario with the change between the stable and unstable modes is always present at the damping ratio defined in Eq. (14).

To better assess the influence of the damping, Fig. 4 shows the stability of the system and the effects of varying the damping ratio $\bar{\mathcal{E}}_1/\bar{\mathcal{E}}_2$ and the frequency ratio $\omega_{0,1}/\omega_{0,2}$ while keeping the friction coefficient and the structural damping $\bar{\mathcal{E}}_2$ at given values. Figure 5 then illustrates the evolution of the associated frequencies. As defined previously, the black and white surfaces (for both the evolution of the frequency and real part) are associated with the stable and unstable static solutions of the merging scenario after the Hopf bifurcation point, respectively. The first general observation from these parametric studies is that increasing the friction coefficient increases the unstable area when the structural damping $\bar{\mathcal{E}}_2$ is constant, as illustrated in Figs. 4(a), 4(b), and 4(d). Moreover, it may be observed that adding damping $\bar{\mathcal{E}}_2$ (for a given ratio damping $\bar{\mathcal{E}}_1/\bar{\mathcal{E}}_2$) increase the stable area when the friction coefficient is constant (see Figs. 4(b) and 4(c)).

Now, considering the evolution of the frequencies (indicated in Fig. 5), the merging scenario when the stable and unstable modes change is detected. This phenomenon is observed when the damping ratio corresponds to Eq. (14). Thus, the value of the damping ratio $\bar{\mathcal{E}}_1/\bar{\mathcal{E}}_2$ plays one of the most important role on the stability of the static point for a mechanical system subject to flutter instability, but also influences the mode coupling behavior and the origin



of the unstable mode.

In conclusion, the role of structural damping is essential and needs to be taken into account. If too much damping is added to only one part of the mechanical system, instability may occur. Therefore, neglecting damping may result in a worse design and a misunderstanding of flutter instability in mechanical systems.

One of the most interesting mechanical processes is that there exist values of the damping ratio ξ_1/ξ_2 for which the merging scenario changes. In some cases, this damping ratio corresponds to the more stable static point of the mechanical system.

Now, the final questions to be answered are: Is it possible to define the optimal damping ratio so that the mechanical system is the more stable system? Is this optimal damping ratio the same as those defined in Eq. (14)? These investigations will be the study of Sec. 4.

4 Robust damping Factor factor

In this section, the definition of the robust damping factor (RD-factor) in order to avoid instability will be investigated. Then numerical examples will be given by considering the previous stability analysis.

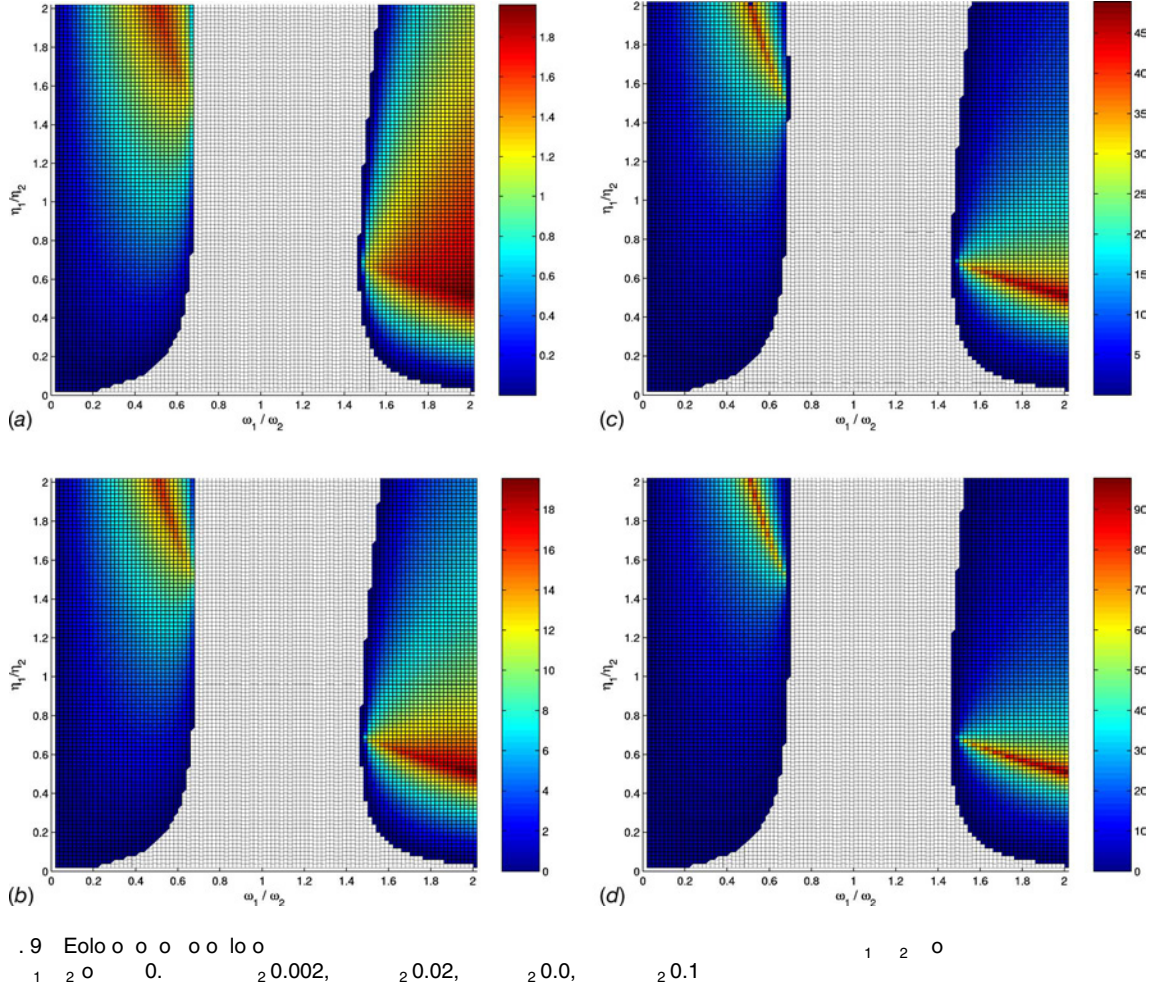
4.1 Definition of the robust damping Factor. In order to define the notion of the robust damping factor, we recall general basic concepts of flutter instability and results previously obtained as follows:

- Neglecting damping in a stability analysis or adding damping on only one part of the system may result in worse design and lead to a misunderstanding of the mode coupling instability of mechanical systems.

- By increasing equal structural damping $c_1=c_2$, the mechanical system is more stable. The evolutions of the real parts of eigenvalues are translated toward the negative real parts. However, the associated frequencies are very little affected by the addition of equal structural damping,
- By increasing nonequal structural damping $c_1 \in c_2$, the mechanical system may be more or less stable than the original one. The evolutions of the real parts of eigenvalues are translated toward the negative real parts. However, the associated frequencies are very little affected by the addition of equal structural damping,
- By introducing various damping ratios, the merging scenario and the unstable mode may change (when $\xi_1/\xi_2 = 0.2/0.1$ i.e., $c_1=c_2$),
- For various structural damping and a given set of parameters, an optimal damping ratio ξ_1/ξ_2 exists. At this point, the stable and unstable modes are reversed,
- Flutter instability is composed of two modes where only one is unstable. For a given set of physical parameters, by increasing the difference between the two frequencies of the stable and unstable modes, the system may be more stable. A decrease of the difference between the stable and unstable frequencies may imply a system more unstable.

Thus, the robust damping factor may be not only a function of the real parts of eigenvalues (that define the stability of the mechanical system) but also the relative values both between the two frequencies of the merging modes.

Then, it was observed that for various given set of parameters, the merging scenario with the change of the stable and unstable



modes appears for equal proportional damping $c_1=c_2$ (see for example Figs. 3(a), 3(b), 4(d), and 5(d)). In others cases, the “optimal damping ratio” (i.e., $c_1=c_2$) does not exist (as illustrated in Figs. 3(c), 3(d), 4(a), 4(b), 5(a), and 5(b)). However, the previous notion of optimal damping ratio may be a good compromise solution if variation of physical parameters are considered. Effectively, Figs. 4(a), 4(b), and 4(d) illustrated the evolution of real parts for a given damping factor $\xi_1=0.1$ and three values of the friction coefficient \forall . For a mechanical system, the friction coefficient may vary. However, this system must be stable for all the possible physical values of the friction coefficient. In this case, the optimal damping ratio, which is an intrinsic constant physical parameter, is a good compromise solution: this solution includes the more stable system for some parameters and a better solution than the undamped system (or some nonequal proportional damping factor for the other cases). This compromise solution corresponds to the case when the difference between the real parts of the two modes

$$R = |\text{Re}(\lambda_{\text{unstable}}) - \text{Re}(\lambda_{\text{stable}})| \quad (15)$$

is zero where $\text{Re}(\lambda)$ defines the real part of λ .

Figure 6(a) shows the variability of $\log(F+1)$ versus the evolutions of the friction coefficient \forall and the damping ratio ξ_1/ξ_2 .

Then, Fig. 7(a) illustrates this variability versus the evolutions of the damping ratio ξ_1/ξ_2 and the frequency ratio $\omega_{0,1}/\omega_{0,2}$. It is clearly observed that the minimum of R corresponds to the merging scenario explained previously.

In order to define the robust damping factor, the associated difference F between the two imaginary parts may be defined by

$$F = |\text{Im}(\lambda_{\text{unstable}}) - \text{Im}(\lambda_{\text{stable}})| \quad (16)$$

where $\text{Im}(\lambda)$ defines the imaginary part of λ .

Figure 6(b) shows the associated variability of $\log(F+1)$ versus the evolutions of the friction coefficient \forall and the damping ratio ξ_1/ξ_2 ; Fig. 7(b) illustrates this variability versus the evolutions of the damping ratio ξ_1/ξ_2 and the frequency ratio $\omega_{0,1}/\omega_{0,2}$. In these cases, it is observed that the minimum of F is obtained when the system is unstable and the merging scenario occurs.

Finally, the RD-factor may be defined by considering two criteria: first, it is defined by the lesser difference between the real parts of the two merging modes (as illustrated in Figs. 6 and 7). We know that this difference is equal to zero when the stable and unstable modes reverse. Second, the robust damping factor corresponds to the greater difference between the two frequencies (for which the associated real parts are equal to zero). Thereby, the criterion of the robust damping factor is defined by

$$\text{RD-factor} = -\max[\text{Re}(\lambda)] \log\left(\frac{F}{R+1} + 1\right) \quad \text{if } \text{Re}(\lambda) > 0$$

$$\text{RD-factor} = 0 \quad \text{if } \text{Re}(\lambda) \leq 0 \quad (17)$$

If the system is unstable, the RD-factor is equal to zero. $-\max[\text{Re}(\lambda)]$ may be defined as the difference between the greater real part of eigenvalues and the zero real-part axis. Thus for a given set of parameters, the greater the proportional structural damping is (i.e., $c_1=c_2$), the greater the RD-factor is, and then the more stable the mechanical system is.

4.2 Application of the robust damping Factor. Now, the notion of the robust damping factor will be now illustrated. Fig-

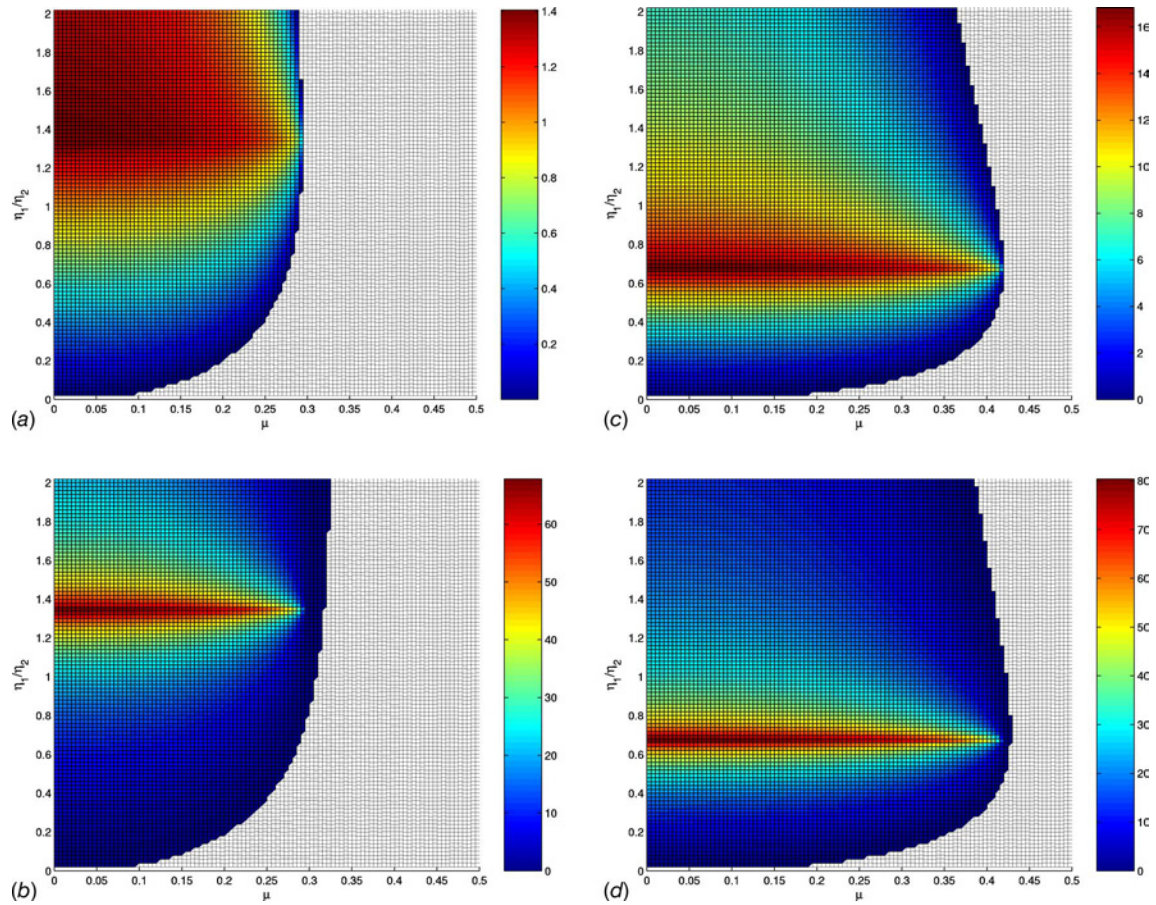


Fig. 10 Variability of the robust damping factor versus the damping ratio ξ_1/ξ_2 and the frequency ratio $\omega_{0,1}/\omega_{0,2}$ for two given values of the friction coefficient \forall . The white surface defines the unstable region of the mechanical system.

ures 8 and 9 show the variability of the robust damping factor versus the damping ratio ξ_1/ξ_2 and the frequency ratio $\omega_{0,1}/\omega_{0,2}$ for two given values of the friction coefficient \forall . The white surface defines the unstable region of the mechanical system.

First of all, it appears that the robust damping factor is greater when the damping ratio ξ_1/ξ_2 corresponds to $\omega_{0,2}/\omega_{0,1}$ (i.e., $c_1 = c_2$) for a given value of the friction coefficient \forall .

Then, the more the system is damped (for a given value of the damping ratio ξ_1/ξ_2), greater the value of the RD-factor is. Thus the RD-factor reflects the fact well that by increasing structural damping, the mechanical system is more stable. In order to avoid design errors and to reduce flutter instability, it is recommended to introduce proportional structural damping and to move the two natural pulsations of the system away. For a given value of the friction coefficient \forall , it appears that the RD-factor indicates the same zone for the most robust damping ratio ξ_1/ξ_2 even if the structural damping ξ_1 varies. This clearly reflects the fact that the estimation of the most suitable damping ratio ξ_1/ξ_2 for friction-induced flutter instability may be determined by using the RD-factor.

Moreover, Fig. 10 illustrates the variability of the robust damping factor versus the damping ratio ξ_1/ξ_2 and the friction coefficient for two given values of the frequency ratio $\omega_{0,1}/\omega_{0,2}$. It may be noted that the damping ratio ξ_1/ξ_2 plays a key role as for the previous study. As explained previously, the RD-factor indicates the same value of the most suitable ratio damping ξ_1/ξ_2 even if the structural damping ξ_1 varies (for a given value of the friction coefficient \forall). In conclusion, the robust damping factor appears to be able to determine the most suitable and robust damping ratio between the stable and unstable modes.

5 Conclusion

It was demonstrated that considering structural damping for mechanical system subject to flutter instability is essential. Increasing or decreasing structural damping may increase or decrease the stable area. The damping ratio between the stable and unstable modes appears to be one of the first factors to take into account to enhance the stability of the system.

The merging scenario of the two modes was examined in detail. It was proved that the damping ratio not only defines the most stable mechanical system, but also influences the merging of the two modes and the origin of the unstable mode.

The notion of the robust damping factor (RD-factor) was introduced in order to define the robust stable mechanical system versus the structural damping factor of the stable and unstable modes. This criterion is a function of the differences between the real parts and imaginary parts of the stable-unstable modes.

References

- [1] Ibrahim, R., 1994, "Friction-Induced Vibration, Chatter, Squeal, and Chaos—Part 2: Dynamics and Modeling," ASME Design Engineering Technical Conference, 7, pp. 227–253.
- [2] Gao, C., Kuhlmann-Wilsdorf, D., and Makel, D., 1994, "The Dynamic Analysis of Stick-Slip Motion," *Wear*, **173**, pp. 1–12.
- [3] Kinkaid, N., O'Reilly, O., and Papadopoulos, P., 2003, "Automotive Disc Brake Squeal," *J. Sound Vib.*, **267**, pp. 105–166.
- [4] Crolla, D., and Lang, A., 1991, "Brake Noise and Vibration—State of Art," *Tribol. Vehicle Tribol.*, **18**, pp. 165–174.
- [5] Earles, S., and Lee, C., 1976, "Instabilities Arising From the Frictional Interaction of a Pin-Disc System Resulting in Noise Generation," *ASME J. Eng. Ind.*, **1**, pp. 81–86.
- [6] Spurr, R., 1961, "A Theory of Brake Squeal," *Proc. Inst. Mech. Eng., Part D (J. Automob. Eng.)*, **1**, pp. 33–40.

- [7] North, M., 1972, "A Mechanism of Disk Brake Squeal," 14th FISITA Congress, Paper No. 1/9.
- [8] Sinou, J.-J., Thouverez, F., and Jézéquel, L., 2004, "Application of a Nonlinear Modal Instability Approach to Brake Systems," *ASME J. Vib. Acoust.*, **126**(1), pp. 101–107.
- [9] Sinou, J.-J., Thouverez, F., and Jézéquel, L., 2003, "Analysis of Friction and Instability by the Center Manifold Theory for a Non-Linear Sprag-Slip Model," *J. Sound Vib.*, **265**(3), pp. 527–559.
- [10] Liu, S., Ozbek, M., and Gordon, J., 1996, "A Nonlinear Model for Aircraft Brake Squeal Analysis. Part II: Stability Analysis and Parametric Studies," *ASME Design Engineering Technical Conference*, 3, pp. 417–425.
- [11] Sinou, J.-J., Dereure, O., Mazet, G.-B., Thouverez, F., and Jézéquel, L., 2006, "Friction Induced Vibration for an Aircraft Brake System. Part I: Experimental Approach and Stability Analysis," *Int. J. Mech. Sci.*, **48**, pp. 536–554.
- [12] Chambrette, P., and Jézéquel, L., 1992, "Stability of a Beam Rubbed Against a Rotating Disc," *Eur. J. Mech. A/Solids*, **11**, pp. 107–138.
- [13] Hoffmann, N., and Gaul, L., 2003, "Effects of Damping on Mode-Coupling Instability in Friction Induced Oscillations," *Z. Angew. Math. Mech.*, **83**(8), pp. 524–534.
- [14] Ibrahim, R., 1994, "Friction-Induced Vibration, Chatter, Squeal, and Chaos. Part I: Mechanics of Contact and Friction," *ASME Design Engineering Technical Conference* 7, pp. 209–226.
- [15] Earles, S., and Chambers, P., 1987, "Disque Brake Squeal Noise Generation: Predicting Its Dependency on System Parameters Including Damping," *Int. J. Veh. Des.*, **8**, pp. 538–552.
- [16] Shin, K., Oh, J.-E., and Brennan, M., 2002, "Nonlinear Analysis of Friction Induced Vibrations of a Two Degree of Freedom Model for Disc Brake Squeal Noise," *JSME Int. J., Ser. A*, **45**, pp. 426–432.
- [17] Shin, K., Brennan, M., Oh, J.-E., and Harris, C., 2002, "Analysis of Disc Brake Noise Using a Two-Degree-of-Freedom Model," *J. Sound Vib.*, **254**, pp. 837–848.
- [18] Sinou, J.-J., and Jézéquel, L., 2007, "Mode Coupling Instability in Friction Induced Vibrations and Its Dependency on System Parameters Including Damping," *Eur. J. Mech. A/Solids*, **26**(1), pp. 106–122.
- [19] Hultén, J., 1993, "Drum Brake Squeal—A Self-Exciting Mechanism With Constant Friction," *SAE Truck and Bus Meeting*, Detroit, Paper No. 932965.
- [20] Hultén, J., 1997, "Friction Phenomena Related to Drum Brake Squeal Instabilities," *SME Design Engineering Technical Conferences*, Sacramento, Paper No. DETC97/VIB-4161.